

1 **Influence of meteorological variability on interannual**
2 **variations of springtime boundary layer ozone over**
3 **Japan during 1981–2005**

4
5 **J. Kurokawa¹, T. Ohara¹, I. Uno², M. Hayasaki³, and H. Tanimoto¹**

6 [1]{National Institute for Environmental Studies, Onogawa, Tsukuba, Ibaraki, Japan}

7 [2]{Research Institute for Applied Mechanics, Kyushu University, Kasuga, Fukuoka,
8 Japan}

9 [3]{Center for Environmental Remote Sensing, Chiba University, Yayoi, Inage, Chiba,
10 Japan}

11 Correspondence to J. Kurokawa (kurokawa.junichi@nies.go.jp)

12
13 **Supplementary Material**

14 **Relationships between springtime BL O₃ over western and central Japan**
15 **and chemical processes**

16 In order to evaluate the influence of chemical processes on the IAV of O₃ over WCJ, we
17 examined the chemical production (P(O₃)), chemical loss (L(O₃)), and net chemical
18 production (N(O₃)) of springtime BL O₃ simulated by E₀₀M_{yy}. P(O₃), L(O₃), and N(O₃)
19 are defined as follows:

20
$$P(O_3) = (k_4[HO_2] + k_5[CH_3O_2] + k_6[RO_2])[NO] \quad (S1)$$

$$\begin{aligned}
21 \quad L(\text{O}_3) &= (k_1 k_2 [\text{H}_2\text{O}] / k_3 [\text{M}] + k_7 [\text{OH}] + k_8 [\text{HO}_2]) [\text{O}_3] \\
22 \quad &+ k_9 [\text{NO}] [\text{O}_3] (k_{11} [\text{NO}_2] [\text{OH}] [\text{M}] / (k_{10} [\text{NO}_2] + k_{11} [\text{NO}_2] [\text{OH}] [\text{M}])) \quad (\text{S2})
\end{aligned}$$

$$23 \quad N(\text{O}_3) = P(\text{O}_3) - L(\text{O}_3) \quad (\text{S3})$$

24 where k_i is the reaction rate coefficient for reaction K_i , listed in Table S1 and M denotes
25 N_2 and O_2 . By running CMAQ, $P(\text{O}_3)$, $L(\text{O}_3)$, and $N(\text{O}_3)$ were obtained every hour; then
26 their springtime BL averages were calculated over East Asia during 1981–2005.

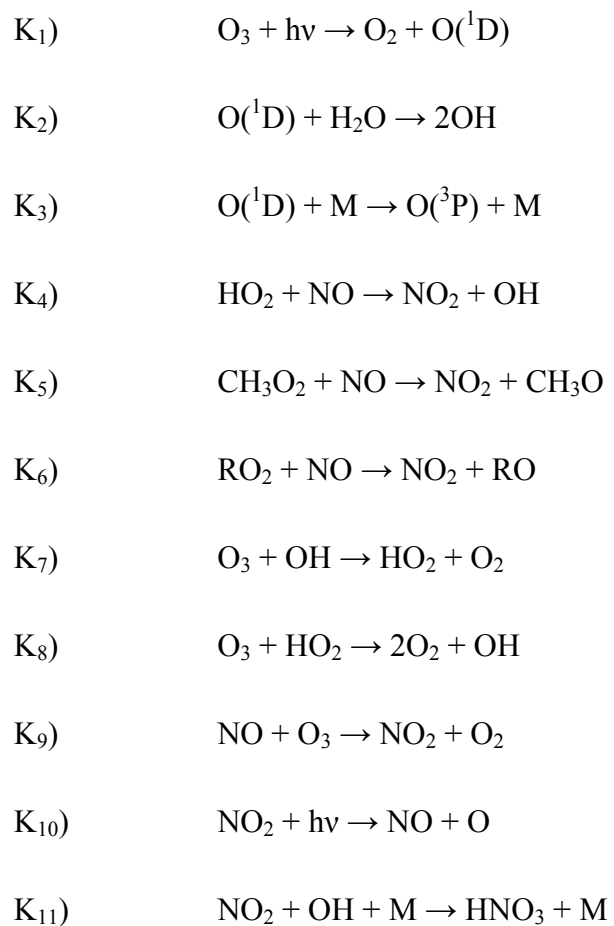
27 Figure S1 shows the composite anomaly fields of springtime BL $P(\text{O}_3)$ (a and b), $L(\text{O}_3)$
28 (c and d), and $N(\text{O}_3)$ (e and f) for high (a, c, and e) and low (b, d, and f) O_3 over WCJ
29 years. During high O_3 over WCJ years, positive anomalies of $P(\text{O}_3)$ were found around
30 the Yangtze Delta and western Japan. On the other hand, large positive anomalies of
31 $L(\text{O}_3)$ (i.e., larger chemical destruction compared to the average) were widespread from
32 the eastern coast of China to south of Japan. This area is almost the same as the region
33 showing positive O_3 anomalies during high O_3 over WCJ years (Fig. 6c). As a result,
34 there were positive anomalies of $N(\text{O}_3)$ over the southern part of WCJ and negative
35 anomalies over the northern part. Relatively large positive $N(\text{O}_3)$ anomalies appeared
36 over the eastern part of CEC, but elsewhere anomalies were small or, over the northern
37 part of CEC, negative. Over the Korean peninsula, anomalies were negative during high
38 O_3 over WCJ years. On the other hand, during low O_3 over WCJ years, anomalies of
39 $P(\text{O}_3)$, $L(\text{O}_3)$, and $N(\text{O}_3)$ showed a very similar horizontal distribution to those during
40 high O_3 over WCJ years but with opposite direction. $N(\text{O}_3)$ anomalies around WCJ
41 were positive in the north and negative in the south. Anomalies of $N(\text{O}_3)$ showed large
42 negative values over the eastern part of CEC, but elsewhere $N(\text{O}_3)$ anomalies showed
43 small negative or positive values. Although clear differences in chemical processes over

44 East Asia are apparent between high and low O₃ over WCJ years, the effects of these
45 processes on the IAV of O₃ are not obvious. Figure S2 displays scatter plots and
46 regression lines (a) between anomalies of springtime BL O₃ and N(O₃) over WCJ and
47 (b) between anomalies of springtime BL O₃ over WCJ and N(O₃) over CEC. Anomalies
48 of O₃ and N(O₃) over WCJ are clearly not related. On the other hand, anomalies of
49 N(O₃) over CEC are positively correlated with those of O₃ over WCJ. However, the
50 slope of regression line is not large and the correlation coefficient is relatively small
51 (0.37). These results suggest that the impact of chemical processes over East Asia on
52 the IAV of O₃ over WCJ is small.

53

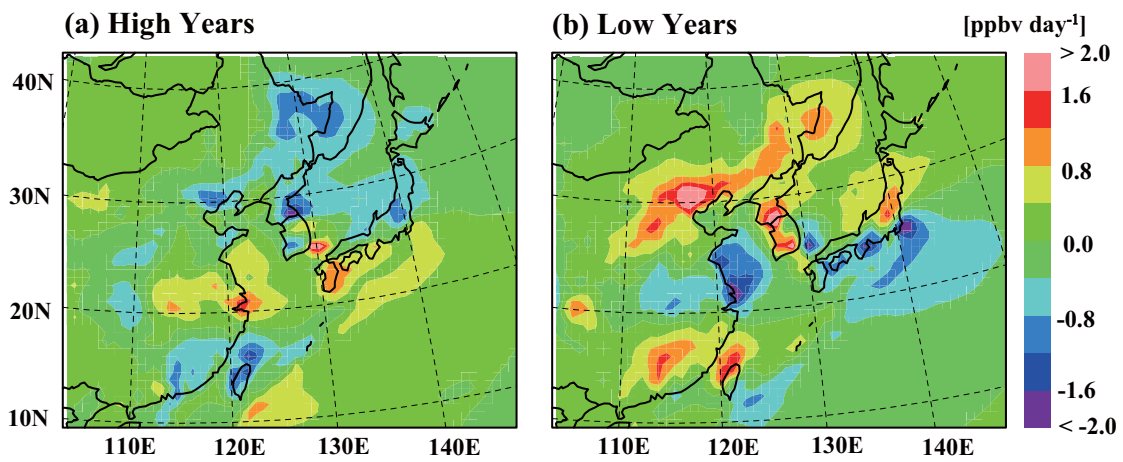
54 Table S1. Reactions in O₃ photochemistry used to calculate P(O₃), L(O₃), and N(O₃).

55

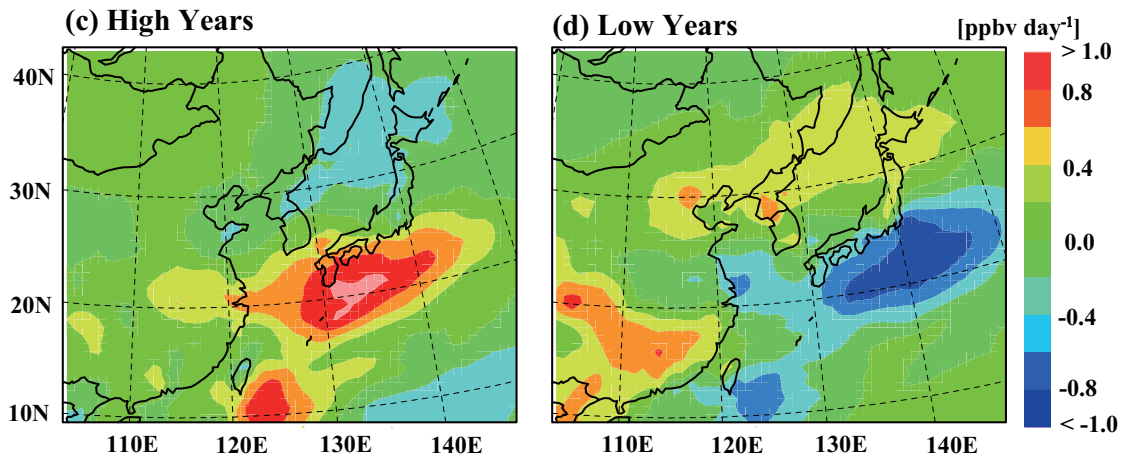


56

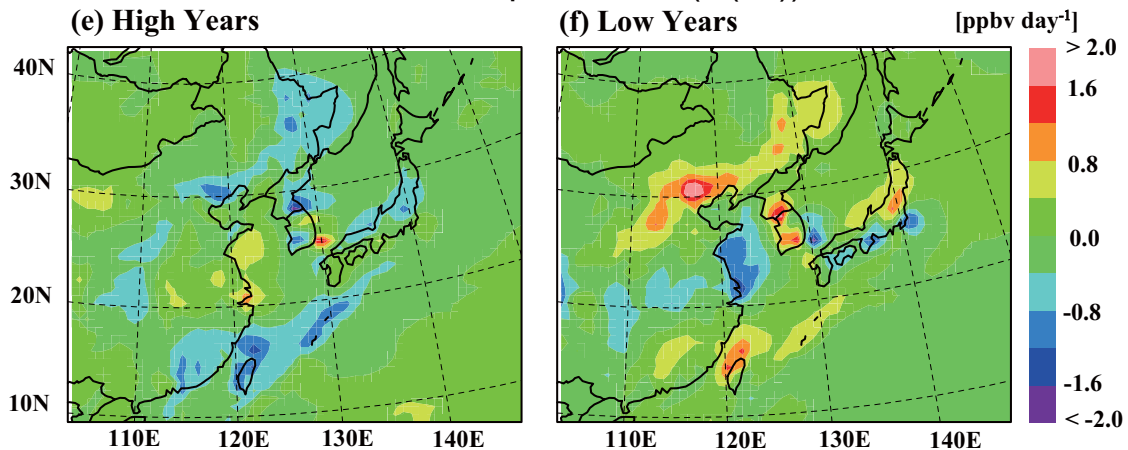
Anomalies of chemical production ($P(O_3)$)



Anomalies of chemical loss ($L(O_3)$)



Anomalies of net chemical production ($N(O_3)$)

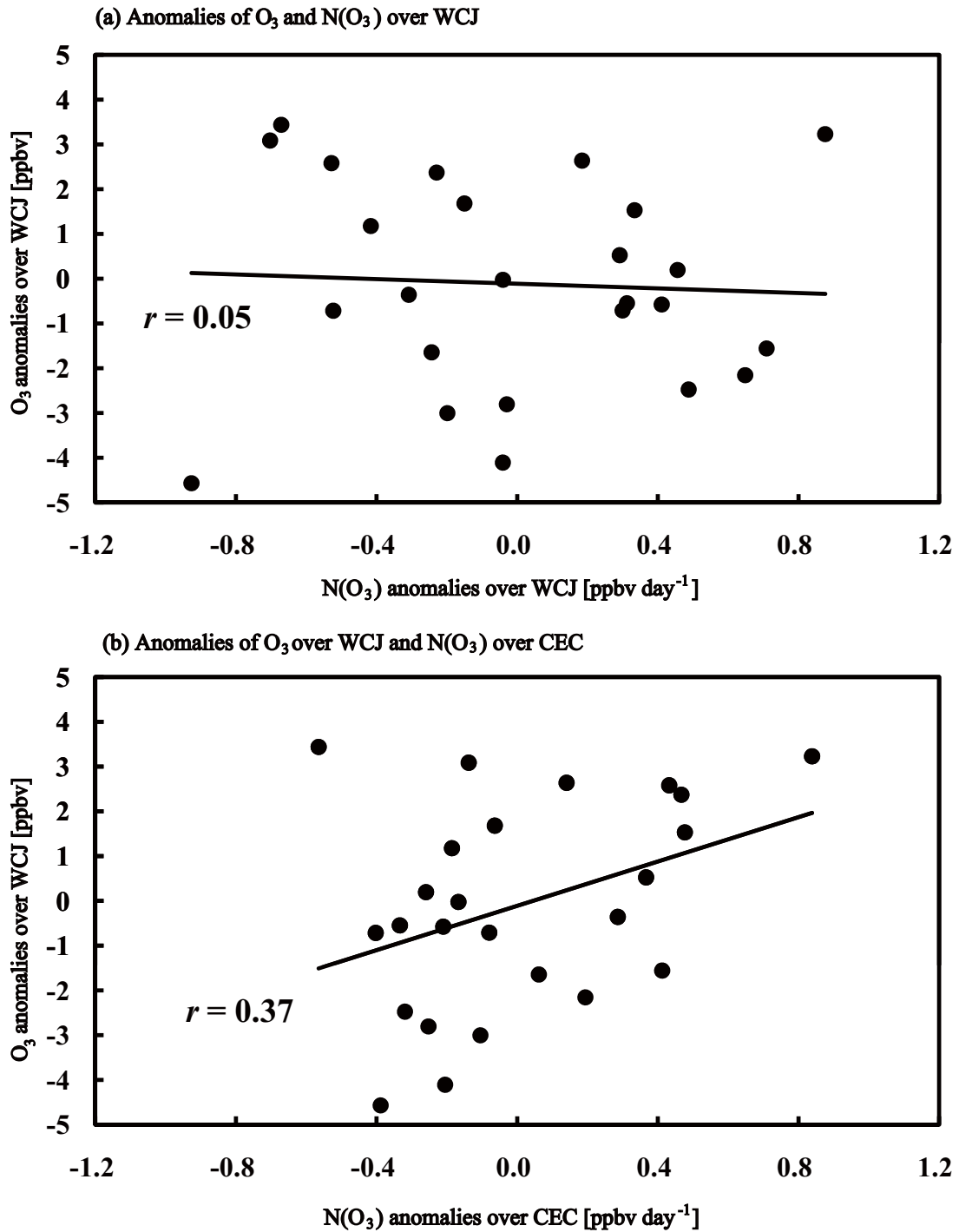


57

58

59 Figure S1. Composite spatial distributions of the anomalies of (a) chemical production
60 ($P(O_3)$), (c) chemical loss ($L(O_3)$), and (e) net chemical production ($N(O_3)$) during high
61 O_3 over WCJ years (High Years). The same information but during low O_3 over WCJ
62 years (Low Years) is shown in (b), (d), and (f), respectively. High (low) O_3 over WCJ
63 years were defined as the top (bottom) 5 years among the springtime BL O_3 anomalies
64 over WCJ between 1981 and 2005. The $E_{00}M_{yy}$ scenario was used for the model
65 simulation. Anomalies are defined as deviations from the averaged values during
66 1981–2005.

67



68

69 Figure S2. (a) Scatter plot and regression line between anomalies of springtime BL O₃
 70 and N(O₃) over WCJ during 1981–2005. (b) The same as in (a) but between anomalies
 71 of springtime BL O₃ over WCJ and N(O₃) over CEC. The simulation scenario and the
 72 definition of anomalies are the same as in Fig. S1.